
Two Behavioral States Studied in a Single PET/FDG Procedure: Theory, Method, and Preliminary Results

Jen Yueh Chang, Ranjan Duara, William Barker, Anthony Apicella,
and Ronald Finn

*Baumritter Institute of Nuclear Medicine, Mount Sinai Medical Center, Miami Beach; and
Departments of Radiology and Neurology, University of Miami, School of Medicine, Miami,
Florida*

We have developed a method that allows two sets of regional cerebral metabolic rates of glucose (rCMRglc) to be obtained in a single extended procedure using positron emission tomography (PET) and [¹⁸F]fluorodeoxyglucose (FDG). This is an adaptation of the deoxyglucose method, with the addition of a second injection of FDG immediately after completion of the first scan, then followed 30 min later by a second scan. A model has been developed to allow for correction of measured tracer concentration in the second scan by subtracting the predicted remnant from the first scan. The possible applications of this method in studying behavior-metabolism relationships are demonstrated. The preliminary results show 6%–12% changes in rCMRglc values for appropriate brain regions when the behavioral state is altered, but show 0%–5% change in rCMRglc values when the behavioral state is unchanged. The method can contribute significantly to the understanding of behavior-metabolism relationships by allowing the noninvasive study of two behavioral states in a single PET procedure.

J Nucl Med 28:852–860, 1987

The deoxyglucose method of measuring regional cerebral metabolic rates of glucose (rCMRglc) (1) has been extensively used in animals with the tracer [¹⁴C]deoxyglucose and autoradiography. In humans, this method has found wide acceptance through the use of tracers, such as [¹⁸F]fluorodeoxyglucose (FDG) and carbon-11 deoxyglucose ([¹¹C]DG), and positron emission tomography (PET) (2,3).

Human studies commonly have been done at resting or baseline states. Yet, it is likely that the applications of PET would be furthered by studying the brain during some form of activation, which may be physiologic, pharmacologic, and/or psychologic (4).

In the commonly used version of the deoxyglucose model (5), the error in the calculation of rCMRglc by PET using [¹⁸F]DG or [¹¹C]DG is reduced by waiting a

minimum of 30 min after the injection of tracer before performing the scan. This minimizes the errors that arise from the use of population rate constants, \bar{K}_1^* , \bar{K}_2^* , and \bar{K}_3^* (5). During the initial 30 min an unchanged behavioral state must persist, because the brain images reflect the regional metabolic activity averaged over this period. Moreover, rapid completion of the scanning sequence is needed to reduce the errors generated by the use of another population rate constant, \bar{K}_1^* (5). The scanning procedure, itself, adds a new and ill-defined behavioral state on the initial state, the effects of which can also be reduced by rapid completion of the scan.

An activation state ideally requires comparison with a control state study, which may be a nonactivation or a specially designed control activation state study on the same subject. This entails repeated PET procedures in a subject, increasing the overall complexity of the method and adding variability to the metabolic values for the two states.

In view of the inconsistencies and the logistical problems that are introduced by repeating PET scans in the same subject at different times, a method that could provide two sets of regional metabolic rates in succes-

Received Jan. 27, 1985; revision accepted Oct. 1, 1986.

For reprints contact: R. Duara, MD, Dept. of Radiology, Mount Sinai Medical Center, Miami Beach, FL 33140.

Preliminary reports of this work were made at the 32nd Annual Meeting of the Society of Nuclear Medicine, Houston, Texas, June 2–5, 1985 and 33rd Annual Meeting of the Society of Nuclear Medicine, Washington, D.C., June 22–25, 1986.

sive epochs without moving the subject out of the scanner, would have several advantages.

We describe here the theory, method, and preliminary results of a procedure that allows calculation of two sets of rCMRglc values representing two distinct behavioral states from a single extended PET study using [¹⁸F]fluorodeoxyglucose.

THEORY AND METHOD

Kinetic Model

The kinetics of FDG transport between blood and brain tissue can be simplified into a three-compartmental model: FDG in plasma, FDG in tissue, and fluorodeoxyglucose-6-phosphate (FDG-6-P) in tissue. The rate constants that govern the transport between the compartments are k_1^* , k_2^* , k_3^* , and k_4^* (Fig. 1), and the concentrations in each compartment are denoted by C_p^* (FDG in plasma), C_e^* (FDG in tissue), and C_m^* (FDG-6-P in tissue). The rate of change for C_e^* and C_m^* in this simplified three-compartmental model, as shown in Figure 1, can be expressed by the following two equations:

$$\frac{d}{dt} C_e^*(t) = k_1^* C_p^*(t) - (k_2^* + k_3^*) C_e^*(t) + k_4^* C_m^*(t) \quad (1)$$

$$\frac{d}{dt} C_m^*(t) = k_3^* C_e^*(t) - k_4^* C_m^*(t). \quad (2)$$

For a steady behavioral state, with stable rate constants from the time of FDG administration to time T_1 , the FDG and FDG-6-P concentration in tissue at time T_1 , $C_e^*(T_1)$ and $C_m^*(T_1)$, can be solved in terms of $C_p^*(t)$ (4).

$$C_e^*(T_1) = \frac{k_1^*}{a_2 - a_1} ((k_4^* - a_1)e^{-a_1 T_1} + (a_2 - k_4^*)e^{-a_2 T_1}) \otimes C_p^*(T_1) \quad (3)$$

$$C_m^*(T_1) = \frac{k_1^* k_3^*}{a_2 - a_1} (e^{-a_1 T_1} - e^{-a_2 T_1}) \otimes C_p^*(T_1), \quad (4)$$

where

$$a_1 = (k_2^* + k_3^* + k_4^* - \sqrt{(k_2^* + k_3^* + k_4^*)^2 - 4k_2^* k_4^*})/2,$$

$$a_2 = (k_2^* + k_3^* + k_4^* + \sqrt{(k_2^* + k_3^* + k_4^*)^2 - 4k_2^* k_4^*})/2,$$

and \otimes denotes the operation of convolution. That is,

$$p(t) \otimes q(t) = \int_0^t p(\tau)q(t - \tau) d\tau.$$

The total amount of ¹⁸F activity in tissue at time T_1 is then the sum of $C_e^*(T_1) + C_m^*(T_1)$; thus,

$$C_e^*(T_1) + C_m^*(T_1) = \frac{k_1^*}{a_2 - a_1} ((k_3^* + k_4^* - a_1)e^{-a_1 T_1} + (a_2 - k_3^* - k_4^*)e^{-a_2 T_1}) \otimes C_p^*(T_1). \quad (5)$$

If at T_1 the steady state changes instantaneously to another steady state, owing to physiologic, psychologic, and/or pharmacologic factors, the FDG transport kinetics between compartments will be adjusted in accordance with the second steady state. Therefore, cerebral FDG uptake from FDG in plasma, FDG phosphorylation, egress of FDG from tissue, and cerebral FDG-6-P dephosphorylation will be governed by a new set of rate constants \hat{k}_1^* , \hat{k}_2^* , \hat{k}_3^* , and \hat{k}_4^* . The rate of tissue FDG and FDG-6-P concentration change will be expressed by the same differential equations as in Eq. (1), but with new rate constants:

$$\frac{d}{dt} C_e^*(t) = \hat{k}_1^* C_p^*(t) - (\hat{k}_2^* + \hat{k}_3^*) C_e^*(t) + \hat{k}_4^* C_m^*(t) \quad (6)$$

$$\frac{d}{dt} C_m^*(t) = \hat{k}_3^* C_e^*(t) - \hat{k}_4^* C_m^*(t). \quad (7)$$

The FDG and FDG-6-P concentration in tissue at any time T_2 (after commencement of the second behavioral state, $T_2 > T_1$) will be $C_e^*(T_2)$ and $C_m^*(T_2)$, and can be solved in terms of $\hat{C}_p^*(t)$ ($\hat{C}_p^*(t) = C_p^*(t + T_1)$), but with the incorporation of the initial condition of C_e^* and C_m^* at T_1 , i.e., $C_e^*(T_1)$ and $C_m^*(T_1)$. Thus,

$$C_e^*(T_2) = \frac{\hat{k}_1^*}{\hat{a}_2 - \hat{a}_1} ((\hat{k}_4^* - \hat{a}_1)e^{-\hat{a}_1(T_2 - T_1)} + (\hat{a}_2 - \hat{k}_4^*)e^{-\hat{a}_2(T_2 - T_1)}) \otimes \hat{C}_p^*(T_2 - T_1) + \frac{\hat{k}_4^* - \hat{a}_1}{(\hat{a}_2 - \hat{a}_1)\hat{k}_3^*} \cdot (C_e^*(T_1)\hat{k}_3^* - (\hat{k}_4^* - \hat{a}_2)C_m^*(T_1))e^{-\hat{a}_1(T_2 - T_1)} + \frac{\hat{k}_4^* - \hat{a}_2}{(\hat{a}_2 - \hat{a}_1)\hat{k}_3^*} ((\hat{k}_4^* - \hat{a}_1)C_m^*(T_1) - C_e^*(T_1)\hat{k}_3^*)e^{-\hat{a}_2(T_2 - T_1)}, \quad (8)$$

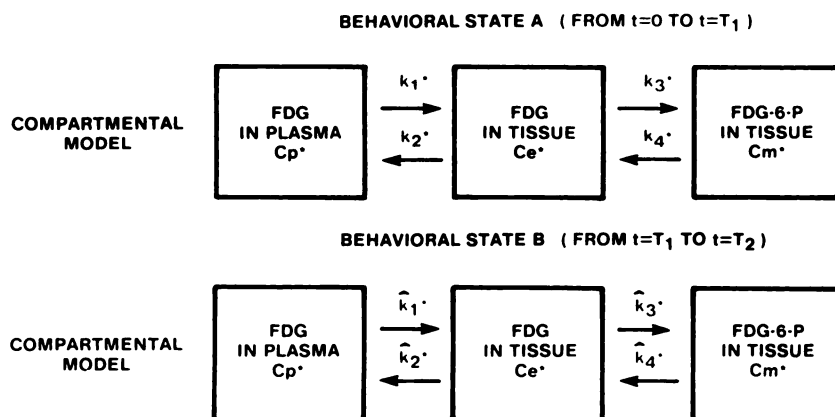


FIGURE 1

Compartmental model used to describe FDG transport between plasma and brain tissue. C_p^* , C_e^* , and C_m^* represent FDG concentration in plasma, FDG concentration in brain tissue, and FDG-6-P concentration in brain tissue, respectively. k_1^* (\hat{k}_1^*) and k_2^* (\hat{k}_2^*) are rate constants governing the transport of FDG between plasma and brain tissue in the first (second) state. k_3^* (\hat{k}_3^*) and k_4^* (\hat{k}_4^*) are the rate constants governing the phosphorylation and dephosphorylation of FDG and FDG-6-P in the first (second) state.

and

$$\begin{aligned}
 & C_m^*(T_2) \\
 &= \frac{\hat{k}_1^* \hat{k}_3^*}{\hat{a}_2 - \hat{a}_1} (e^{-\hat{a}_1(T_2-T_1)} - e^{-\hat{a}_2(T_2-T_1)}) \otimes \hat{C}_p^*(T_2 - T_1) \\
 &+ \frac{1}{\hat{a}_2 - \hat{a}_1} (C_e^*(T_1) \hat{k}_3^* - (\hat{k}_4^* - \hat{a}_2) C_m^*(T_1)) e^{-\hat{a}_1(T_2-T_1)} \quad (9) \\
 &+ \frac{1}{\hat{a}_2 - \hat{a}_1} ((\hat{k}_4^* - \hat{a}_1) C_m^*(T_1) - C_e^*(T_1) \hat{k}_3^*) e^{-\hat{a}_2(T_2-T_1)}.
 \end{aligned}$$

The total amount of activity at T_2 is the sum of $C_e^*(T_2)$ and $C_m^*(T_2)$. After rearranging the terms, $C_e^*(T_2) + C_m^*(T_2)$ can be expressed as follows:

$$\begin{aligned}
 & C_e^*(T_2) + C_m^*(T_2) \\
 &= \frac{\hat{k}_1^*}{\hat{a}_2 - \hat{a}_1} ((\hat{k}_3^* + \hat{k}_4^* - \hat{a}_1) e^{-\hat{a}_1(T_2-T_1)} \\
 &+ (\hat{a}_2 - \hat{k}_3^* - \hat{k}_4^*) e^{-\hat{a}_2(T_2-T_1)}) \otimes \hat{C}_p^*(T_2 - T_1) \quad (10) \\
 &+ \frac{1}{\hat{a}_2 - \hat{a}_1} (C_e^*(T_1) + C_m^*(T_1)) (\hat{a}_2 e^{-\hat{a}_1(T_2-T_1)} \\
 &- \hat{a}_1 e^{-\hat{a}_2(T_2-T_1)}) - \frac{\hat{k}_2^* C_e^*(T_1)}{\hat{a}_2 - \hat{a}_1} (e^{-\hat{a}_1(T_2-T_1)} - e^{-\hat{a}_2(T_2-T_1)}).
 \end{aligned}$$

By denoting $R^*(T_2:T_1)$ as the difference between the second and third terms in the right side of Eq. (10), and $C_e^*(T_2:T_1)$ as the result of $C_e^*(T_2) + C_m^*(T_2)$ minus $R^*(T_2:T_1)$, Eq. (10) can be rewritten as:

$$\begin{aligned}
 & C_e^*(T_2:T_1) \\
 &= C_e^*(T_2) + C_m^*(T_2) - R^*(T_2:T_1) \\
 &= \frac{\hat{k}_1^*}{\hat{a}_2 - \hat{a}_1} ((\hat{k}_3^* + \hat{k}_4^* - \hat{a}_1) e^{-\hat{a}_1(T_2-T_1)} \\
 &+ (\hat{a}_2 - \hat{k}_3^* - \hat{k}_4^*) e^{-\hat{a}_2(T_2-T_1)}) \otimes \hat{C}_p^*(T_2 - T_1), \quad (11a)
 \end{aligned}$$

where

$$\begin{aligned}
 R^*(T_2:T_1) &= \frac{1}{\hat{a}_2 - \hat{a}_1} (C_e^*(T_1) + C_m^*(T_1)) \\
 &\cdot (\hat{a}_2 e^{-\hat{a}_1(T_2-T_1)} - \hat{a}_1 e^{-\hat{a}_2(T_2-T_1)}) \\
 &- \frac{\hat{k}_2^* C_e^*(T_1)}{\hat{a}_2 - \hat{a}_1} (e^{-\hat{a}_1(T_2-T_1)} - e^{-\hat{a}_2(T_2-T_1)}). \quad (11b)
 \end{aligned}$$

The right side of Eq. (11a), then, has the same expression as the right side of Eq. (5), implying that $C_e^*(T_2:T_1)$ is the tracer concentration at T_2 that was accumulated from FDG in plasma during the second steady state, utilizing the new set of rate constants. $R^*(T_2:T_1)$ is the remnant of the tracer concentration in tissue from T_1 at T_2 , and can be obtained from $C_e^*(T_1) + C_m^*(T_1)$ using Eq. (11b), with the respective rate constants. Whereas, $C_e^*(T_2:T_1)$ can be obtained by subtracting $R^*(T_2:T_1)$ from $C_e^*(T_2) + C_m^*(T_2)$.

The ratio of $C_e^*(T_2:T_1)$ to $R^*(T_2:T_1)$ is related to the concentration of tracer at T_1 and T_2 , and to the time interval between T_1 and T_2 . For example, if no additional tracer were administered after T_1 and $T_2 - T_1 = 50$ min, the ratio will be about 0.7, which is the remnant of tracer, after physical decay. The ratio can be improved significantly, however, by admin-

istering additional tracer after T_1 . If the additional amount of tracer injected is equal in dose to that in the first injection, the ratio improves to 2.6. Even further improvement can be achieved by administering greater amounts of tracer after T_1 .

CMRglc Calculation Using PET

In the steady state, the metabolic rate for glucose in a brain region can be calculated by the following equation:

$$rCMRglc = \frac{Cp k_1^* k_3^*}{LC(k_2^* + k_3^*)}, \quad (12)$$

where Cp is the plasma glucose concentration and LC is the lumped constant (I). Unfortunately, to solve Eq. (12) the rate constants for every brain region have to be measured in Eq. (12). Therefore, Sokoloff et al. (1) adopted an operational equation and used average rate constant values to determine $rCMRglc$ autoradiographically. Huang et al. (4) modified this equation to include the dephosphorylation rate constant (k_4^*). Later, Hutchins et al. (6) further modified the equation to reduce the error sensitivity of $rCMRglc$ to the rate constants, and the operational equation became as follows:

$$rCMRglc = \frac{Cp \bar{k}_1^* \bar{k}_3^*}{LC(\bar{k}_2^* + \bar{k}_3^*)} \frac{C^*(T_1)}{C_e^*(T_1) + \bar{C}_m^*(T_1)}, \quad (13)$$

where \bar{k}_1^* , \bar{k}_2^* , \bar{k}_3^* , and \bar{k}_4^* are average rate constant values from normal volunteers, $C^*(T_1)$ is the regional ^{18}F activity concentration in tissue at T_1 measured by PET, and $\bar{C}_e^*(T_1)$ and $\bar{C}_m^*(T_1)$ are estimated concentrations of FDG and FDG-6-P in tissue, based on predicted DG transport mechanisms using average rate constant values and the measured plasma FDG activity. If the regional cerebral ^{18}F concentration that is accumulated from FDG in plasma, during any particular behavioral state, and the history of FDG concentration in plasma can be obtained, this simplified operational equation can be used to estimate the $rCMRglc$ for that state and Eq. (13) can then be generalized as follows:

$$rCMRglc = \frac{Cp \bar{k}_1^* \bar{k}_3^*}{LC(\bar{k}_2^* + \bar{k}_3^*)} \frac{C_e^*(T_f:T_i)}{\bar{C}_e^*(T_f:T_i) + \bar{C}_m^*(T_f:T_i)}, \quad (14)$$

$$C_e^*(T_f:T_i) = C^*(T_f) - R^*(T_f:T_i),$$

where T_i is the time of commencement and T_f is the time of completion of that state. $\bar{C}_e^*(T_f:T_i)$ and $\bar{C}_m^*(T_f:T_i)$ are the estimated concentrations of FDG and FDG-6-P in tissue, accumulated from FDG in plasma between time T_i and T_f . $C^*(T_f)$ is the ^{18}F activity concentration at T_f , and $R^*(T_f:T_i)$ is the remnant of tracer concentration in tissue from T_i at T_f . When T_f and T_i are replaced by T_1 and 0, $R^*(T_2:T_1)$ will be equal to 0, and Eq. (13) becomes a special case of Eq. (14).

$rCMRglc$ of the initial steady state is calculated using operational Eq. (13). [$C^*(T_1)$ is determined from the first 20-min PET scan (Fig. 2)]. Determination of $rCMRglc$ for the second state requires the value for $R^*(T_2:T_1)$, which cannot be obtained directly, but can be estimated from its relationship to $C_e^*(T_1)$, $C_m^*(T_1)$, $C_e^*(T_2)$, and $C_m^*(T_2)$, as shown in Eq. (11b). This estimation poses two difficulties: (a) The individual rate constants are not available for this adapted PET autoradiographic method, and (b) because PET measures only the total ^{18}F activity, $C^*(t)$, in tissue, the sum of $C_e^*(t)$ and $C_m^*(t)$ in Eq. (13) can be determined, but not the individual values of $C_e^*(t)$ or $C_m^*(t)$. Therefore, averaged rate constant values are needed in the estimation process. By inserting average rate

constant values in Eq. (11b) and rearranging the terms, the approximate value of $R^*(T_2:T_1)$, $\bar{R}^*(T_2:T_1)$, is expressed as follows:

$$\bar{R}^*(T_2:T_1) = C^*(T_1)(\bar{A}^*(T_2:T_1) - \bar{B}^*(T_2:T_1)), \quad (15)$$

where

$$\bar{A}^*(T_2:T_1)$$

$$= \left(\frac{\bar{a}_2}{(\bar{a}_2 - \bar{a}_1)} - \frac{K_2^* \bar{C}_c^*(T_1)}{(\bar{a}_2 - \bar{a}_1)(\bar{C}_c^*(T_1) + \bar{C}_m^*(T_1))} \right) e^{-\bar{a}_1(T_2 - T_1)}$$

$$\bar{B}^*(T_2:T_1)$$

$$= \left(\frac{\bar{a}_1}{(\bar{a}_2 - \bar{a}_1)} - \frac{K_2^* \bar{C}_c^*(T_1)}{(\bar{a}_2 - \bar{a}_1)(\bar{C}_c^*(T_1) + \bar{C}_m^*(T_1))} \right) e^{-\bar{a}_2(T_2 - T_1)}$$

derived using average rate constant values.

The calculation of the approximate value of $C^*(T_2:T_1)$, $\bar{C}_c^*(T_2:T_1)$, is as follows: The two constants, $\bar{A}^*(T_2:T_1)$ and $\bar{B}^*(T_2:T_1)$ as described earlier, are first calculated using average rate constant values and the history of tracer concentration between $t = 0$ and $t = T_1$. Then $C^*(T_1)$ is multiplied by the result of $\bar{A}^*(T_2:T_1) - \bar{B}^*(T_2:T_1)$, according to Eq. (15) to determine $\bar{R}^*(T_2:T_1)$. Finally, $\bar{R}^*(T_2:T_1)$ is subtracted from $C^*(T_2)$ giving the value $\bar{C}_c^*(T_2:T_1)$. Provided that the subject's head remains in the same position during the entire study, the corresponding pixels from each PET image represent identical tissue locations. The subtraction of $\bar{R}^*(T_2:T_1)$ from $C^*(T_2)$ is then performed pixel by pixel, generating $\bar{C}_c^*(T_2:T_1)$. Finally, CMRglc for the second state can be obtained using Eq. (14).

FDG Preparation

FDG was synthesized by the Mount Sinai Medical Center radiochemistry and cyclotron staff, using the fluoride ion (F^-) and the nucleophilic displacement reaction (7) modified for multimillicurie levels (8), and free of [^{18}F]2-fluoro-2-deoxy-D-mannose. The purity of the radiopharmaceutical has been confirmed (9).

Human Studies

Subjects abstained from use of all medications, coffee, tea, cigarettes, and alcohol for 24 hr prior to the scan and fasted for at least 4 hr before the study to stabilize blood glucose levels and enhance FDG uptake. A hand was warmed in a

Lucite chamber with air temperature maintained at 45°–50°C. This served to arterialize venous blood. Blood samples were obtained from the dorsal vein of a heated hand. The sequence of injection/activation/scan is illustrated in Figure 2. The activation was started approximately 2 min prior to the FDG injection. Following a bolus administration of 3–4 mCi of FDG injected intravenously, the first selected behavioral task was performed by the patient for 30 min. Then the subject's head was positioned in the PET camera, with the plane of scanning parallel to the inferior orbito-meatal line, and scanning proceeded over 20 min. This was immediately followed by commencement of the second specific task. Two minutes after the onset of this task, a second bolus of FDG was injected, which equalled the first in dose. Activation was again continued for 30 min. The head position was rechecked before rescanning, which proceeded over the next 20 min. An average of 1–3 million counts per slice were obtained for the first scan and 3–5 million counts per slice were obtained for the second scan. Following each injection of FDG, heated venous blood was drawn at 10-sec intervals in the first 2 min after the FDG injection; then the sampling interval was gradually increased to 5 min. Blood samples were transferred into heparinized and fluorinated vials and placed on ice immediately after withdrawal, to stop further biochemical reaction. Plasma was separated for the determination of plasma glucose and radioactivity levels. Plasma glucose was measured by standard enzymatic techniques, while radioactivity in plasma was determined by counting 0.200-ml samples of plasma in a gamma counter.

Regional brain radioactivity levels were measured by a modified PETT V positron emission tomograph machine, capable of obtaining seven simultaneous brain slices of 14–18 mm thickness, with inplane resolution of 15 mm (full width at half maximum) and a sensitivity of 165,000 cps/ μ Ci/cc. An analytical attenuation correction, that assumes the head is elliptical and homogeneous, was performed on the projection data.

PET scans were analyzed, by methods described previously, to obtain metabolic data for up to 63 regions of interest (10). For the purposes of this study, results for individual brain regions were averaged for specific lobules (Appendix 1).

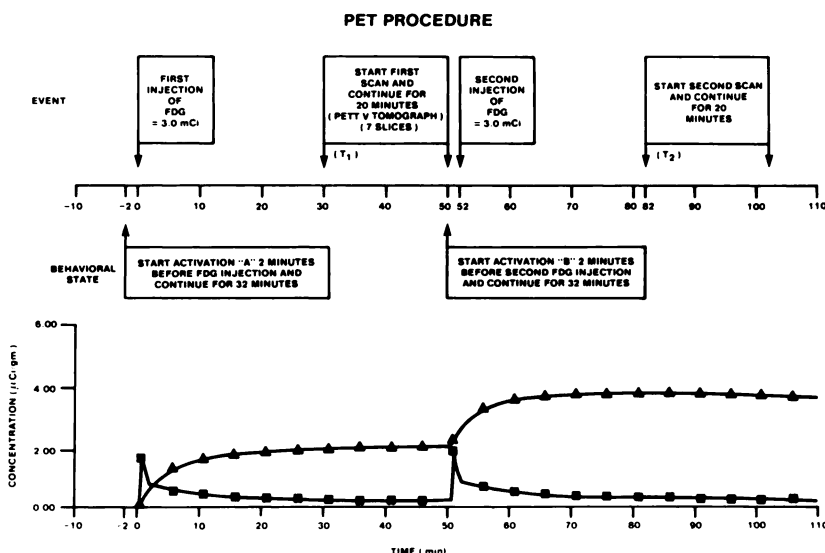
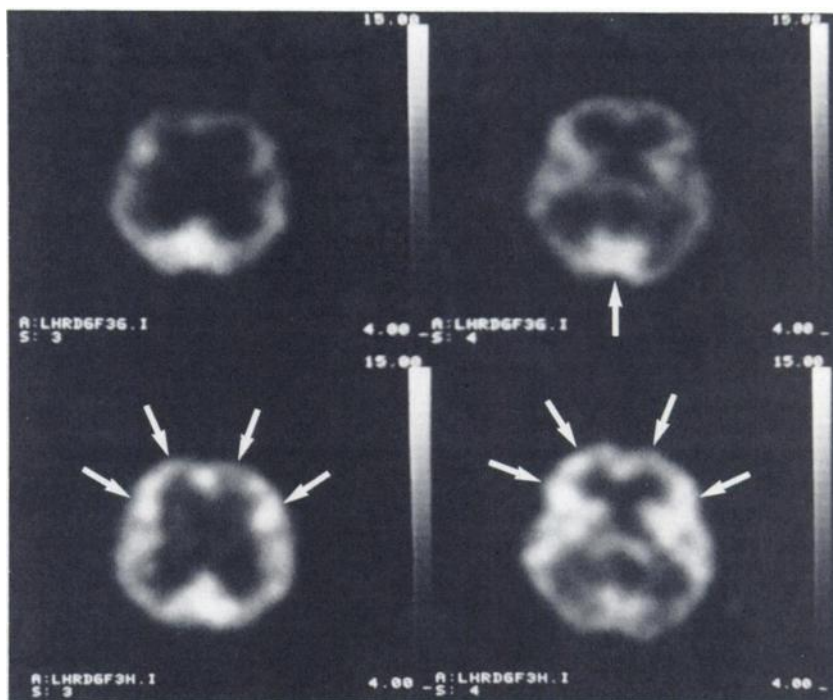


FIGURE 2
Time relations of the behavioral and physiological events for the overall procedure. (Δ) Brain concentration of tracer; (\blacksquare) Plasma concentration of tracer.

FIGURE 3

Fig. 3a shows two levels of brain (slices 3 and 4) for Subject 4, representing the first behavioral state (PPT). Arrow points to occipital cortex activation. Fig. 3b shows the same two levels of brain for Subject 4 representing the second behavioral state (WFT). Arrows point to frontal lobe activation.



Before the analysis of the data for the second state in each study, it was necessary to determine that there had been no movement of the subject's head, relative to the scanner, between the first and second states. This was confirmed by comparing the outlines of, and details within, the scans for each of seven slices.

Psychologic Activation Procedure

To demonstrate the utility of this method certain combinations of behavioral activation tasks were chosen for this study. Two activation procedures were used, namely, an adaptation of the Thurstone Word Fluency Test (WFT) (11) and a picture preference test (PPT). Poor performance on WFT has been associated with frontal lobe lesions in a variety of studies (12-14). Earlier studies performed in this laboratory have indicated that the Thurstone Word Fluency Test, modified so it can be administered over a 30-min period, causes greater frontal than occipital activation (15). Subjects were required to say as many words as possible that began with a given letter of the alphabet. One minute was allowed per letter. The task was continued for 30 min. During the task the subject's eyes were closed and ears were plugged.

The picture preference test required the subject to view colored slides of landscapes, seascapes, animals, faces, and inanimate objects, projected for 4 sec each. The subjects were required to look at the pictures continuously and indicate whether or not they liked each picture by pressing a response button in the right or left hand. The PPT was used in this study to activate the primary and associative visual cortex.

Reproducibility of cerebral metabolic values from the second behavioral state to the values from the first behavioral state by this double activation/double injection method were examined. Five and four subjects, respectively, repeatedly performed either PPT or WFT. Differences in regional metabolic rates for the repeated tasks were calculated.

Cerebral metabolic values for two different behavioral tasks,

studied by this method, were also analyzed. These subjects ($n = 4$) had PPT following the first injection, and WFT following the second injection. All subjects participating in these studies were healthy normal volunteers.

In addition, data are presented for four healthy subjects who had PPT and another four subjects who had WFT administered in the 30-min activation period of the traditional single injection deoxyglucose method. These data are used to show how the results from the double injection modification compares with the single injection deoxyglucose method.

RESULTS

Metabolic data are reported here using the kinetic model described earlier. The precision and accuracy of this double injection/double activation method were measured by the following means: (a) the reproducibility of regional metabolic values was examined when the same behavioral task was repeated after the first and the second injections; (b) the differences in regional metabolic rates were examined when different behavioral tasks (PPT and WFT) were used after the first and second injections; (c) the differences in regional metabolic rates were examined in two separate groups of subjects, one of which had PPT and one of which had WFT. These studies were performed by the standard, single injection, deoxyglucose method.

Tables 1 and 2 show the reproducibility of rCMRglc values when PPT and WFT, respectively, were repeated. For PPT the unsigned mean delta percent (mean absolute percent difference of rCMRglc values from behavioral state 1 to behavioral state 2) across each lobule was 1.4% and mean s.d. was 6.2%. The range of regional

changes was from -5.1% to 1.7%. For WFT the mean unsigned delta percent across each lobule was 2.0% and mean s.d. was 4.2%. The range of regional changes was from -4.8% to 2.5%.

Table 3 shows the mean delta percent and its s.d. in rCMRglc values when PPT and WFT were used sequentially as activating tasks after the first and second injections, respectively. Nine of 24 lobules showed significant differences of metabolic values between the two standard states (paired t-test, $p < 0.05$). Metabolic values were higher in bilateral prefrontal (6%), left premotor (13%), right premotor (8%), and deep gray matter structures (6%) during WFT than during PPT, whereas, occipital metabolic values were higher on the right (11%) and left (9%) sides during PPT, relative to WFT. The metabolic value alteration (1.5%) in the right orbitofrontal region was statistically significant but probably not of real importance because of the small magnitude of change.

Table 4 shows relative regional metabolic values (ratios of rCMRglc to mean gray matter CMRglc) for two groups of subjects in whom metabolic rates were calculated by the standard single injection method. In Group 1 the activation was PPT and in Group 2 the activation was WFT. We used relative metabolic values

TABLE 1
Reproducibility of Metabolic Values for Double Activation/
Double Injection Method

Picture preference - picture preference (n = 5, age = 50 ± 8 yr)	
Lobules	Δ% rCMRglc ± s.d.
Right prefrontal	0.4 ± 6.2
Left prefrontal	0.3 ± 5.3
Right premotor	-3.1 ± 6.0
Left premotor	-2.6 ± 5.1
Right orbito-frontal	-4.4 ± 6.5
Left orbito-frontal	-5.1 ± 6.7
Right motor	0.9 ± 6.1
Left motor	-0.5 ± 5.7
Right sensory	-1.6 ± 8.6
Left sensory	1.5 ± 6.2
Right superior parietal	0.4 ± 7.5
Left superior parietal	0.9 ± 3.4
Right inferior parietal	-2.0 ± 5.1
Left inferior parietal	-1.2 ± 4.4
Right superior temporal	0.8 ± 5.9
Left superior temporal	-1.7 ± 3.7
Right medial temporal	-0.5 ± 7.7
Left medial temporal	0.7 ± 5.4
Right deep gray	-0.5 ± 8.6
Left deep gray	1.4 ± 5.7
Right occipital	0.7 ± 7.0
Left occipital	0.7 ± 6.8
Right cerebellum	-1.3 ± 7.0
Left cerebellum	-0.8 ± 5.4
Unsigned mean Δ% and mean s.d.	1.4 ± 6.2

TABLE 2
Reproducibility of Metabolic Values for Double Activation/
Double Injection Method

Word fluency - word fluency (n = 4, age = 71 ± 5 yr)	
Lobules	Δ% rCMRglc ± s.d.
Right prefrontal	-1.8 ± 4.1
Left prefrontal	0.9 ± 4.5
Right premotor	-3.0 ± 3.6
Left premotor	-2.4 ± 0.9
Right orbito-frontal	-1.7 ± 4.5
Left orbito-frontal	-2.8 ± 0.9
Right motor	-3.1 ± 3.4
Left motor	-0.4 ± 5.5
Right sensory	-1.6 ± 3.3
Left sensory	0.2 ± 8.2
Right superior parietal	-0.7 ± 5.7
Left superior parietal	1.4 ± 8.5
Right inferior parietal	-2.5 ± 3.0
Left inferior parietal	-2.9 ± 3.8
Right superior temporal	-4.3 ± 1.2
Left superior temporal	-4.8 ± 3.6
Right medial temporal	-2.6 ± 3.8
Left medial temporal	-0.9 ± 4.2
Right deep gray	1.4 ± 7.0
Left deep gray	2.5 ± 6.8
Right occipital	-1.6 ± 3.5
Left occipital	-0.5 ± 3.5
Right cerebellum	-1.6 ± 4.8
Left cerebellum	-1.7 ± 2.5
Unsigned mean Δ% and mean s.d.	2.0 ± 4.2

because these show considerably less interindividual variation than rCMRglc values, which have a coefficient of variation of ~18%-28% (5). To assess the significance of regional differences between Groups 1 and 2 we used t-tests. Only the occipital regions, the right cerebellum, and left superior parietal region showed differences at $p < 0.05$ level. The right and left occipital regions had higher values during PPT by 15% and 12%, respectively. The right cerebellum had higher values by 18% during WFT. The left superior parietal region had higher values by 10% during PPT.

There is partial agreement using our double injection/double activation method and the standard deoxyglucose/single injection method. Because the double injection method uses rCMRglc values and intraindividual comparisons in sequential scans and the standard single injection method uses relative regional metabolic values and interindividual comparisons, the double injection method is likely to be more sensitive to real differences. Both methods demonstrate that PPT activates the occipital lobes, but only the double injection method reveals premotor, and deep gray matter structures to be activated during WFT. These structures are known to be activated during WFT from other standard single injection deoxyglucose studies that we have performed comparing WFT with the resting state (15,16).

From these preliminary results it can be seen that, when the same task is repeated, there are very small differences in metabolic values. When different tasks are used, however, specific brain lobules show significant differences of metabolic values. Because these changes are averaged over a whole lobule (Appendix 1), specific regions within the lobules may change to a greater extent.

DISCUSSION

We have demonstrated that a simple adaptation of the deoxyglucose method (1), using [18-F] fluorodeoxyglucose and PET, allows the measurement of regional metabolic rates for two behavioral states. Provision of data for the additional behavioral state, 30–40 min after the first, may considerably enhance the understanding of behavior–metabolism relationships. Results of a baseline or control state are useful for the adequate interpretation of metabolic data from a specific behavioral state. Because the subject does not have to be moved out of the scanner between the two measurements, accurate repositioning of the head is easily obtained. The short time interval between the

TABLE 3
Difference in Metabolic Values for Two Different Behavioral Tasks by Double Activation/Double Injection Method

Picture preference – word fluency (n = 4, age = 62 ± 15 yr)	
Lobule	Δ% rCMRglc ± s.d.
Right prefrontal	-6.2' ± 2.4
Left prefrontal	-6.1' ± 2.0
Right premotor	-7.8' ± 4.4
Left premotor	-12.6' ± 6.9
Right orbito-frontal	-1.5' ± 0.7
Left orbito-frontal	-2.9 ± 2.7
Right motor	-4.1 ± 6.0
Left motor	-7.8 ± 7.5
Right sensory	-1.7 ± 5.0
Left sensory	-4.9 ± 6.8
Right superior parietal	-2.4 ± 4.2
Left superior parietal	-4.0 ± 3.9
Right inferior parietal	5.6 ± 11.6
Left inferior parietal	-0.6 ± 7.5
Right superior temporal	-0.8 ± 3.8
Left superior temporal	-2.2 ± 4.1
Right medial temporal	1.4 ± 6.6
Left medial temporal	-1.3 ± 6.1
Right deep gray	-6.3' ± 3.0
Left deep gray	-5.6' ± 3.8
Right occipital	11.0' ± 7.0
Left occipital	9.0' ± 4.0
Right cerebellum	-2.1 ± 7.4
Left cerebellum	0.2 ± 4.2

' Paired t-test, p < 0.05.

TABLE 4
Differences in Metabolic Values for Two Different Behavioral Tasks in Separate Subject Groups by Standard Deoxyglucose Method

Lobule	Group 1 (n = 4, age = 62 ± 15 yr) (picture preference)	Group 2 (n = 4, age = 68 ± 11 yr) (word fluency)
	(rCMRglc/̄rCMRglc' ± s.d.	(rCMRglc/̄rCMRglc ± s.d.
Right prefrontal	0.98 ± 0.04	0.98 ± 0.05
Left prefrontal	0.97 ± 0.03	0.97 ± 0.05
Right premotor	1.03 ± 0.10	1.10 ± 0.02
Left premotor	1.03 ± 0.05	1.07 ± 0.03
Right orbito-frontal	0.95 ± 0.07	0.88 ± 0.06
Left orbito-frontal	0.95 ± 0.05	0.87 ± 0.05
Right motor	1.06 ± 0.03	1.06 ± 0.11
Left motor	1.02 ± 0.01	1.06 ± 0.10
Right sensory	1.03 ± 0.02	1.00 ± 0.09
Left sensory	1.00 ± 0.08	1.02 ± 0.06
Right superior parietal	0.98 ± 0.04	0.92 ± 0.08
Left superior parietal	0.98' ± 0.05	0.88 ± 0.05
Right inferior parietal	1.04 ± 0.05	1.00 ± 0.04
Left inferior parietal	0.99 ± 0.06	0.98 ± 0.06
Right superior temporal	0.98 ± 0.04	1.01 ± 0.02
Left superior temporal	0.93 ± 0.05	0.98 ± 0.06
Right medial temporal	0.84 ± 0.08	0.95 ± 0.08
Left medial temporal	0.83 ± 0.07	0.95 ± 0.07
Right deep gray	1.01 ± 0.04	1.08 ± 0.04
Left deep gray	1.03 ± 0.04	1.09 ± 0.06
Right occipital	1.16 [†] ± 0.09	1.01 ± 0.04
Left occipital	1.13 [†] ± 0.08	1.01 ± 0.03
Right cerebellum	0.93 [†] ± 0.06	1.11 ± 0.05
Left cerebellum	0.96 ± 0.08	1.05 ± 0.08

* Ratio of regional glucose metabolic rate to mean gray matter metabolic rate.

[†] p < 0.05 (t-test).

two measurements also makes for improved comparability between the two states.

Certain other advantages to this adaptation of the standard deoxyglucose method become apparent. Because two separate studies in each subject are no longer necessary, the total time involvement for the subject is almost halved. For the investigator, the effort directed to a single patient is almost halved. These factors improve the efficiency of FDG/PET studies, provided it is accepted that two behavioral studies are desirable on each subject.

We have not as yet presented data that would allow quantitative assessment of the degree of activation when a task is performed in the first 30-min versus the second

APPENDIX 1
Combinations of Brain Regions in Each Lobule

Brain regions [†]	mm Above IOM line [†]	Lobules
Superior frontal	80–100	Prefrontal
Superior frontal	60–80	
Superior frontal	35–60	Premotor
Mid frontal	65–90	
Mid frontal	45–65	
Inferior frontal	50–70	
Inferior frontal	35–50	Orbito-frontal
Orbito-frontal	20–35	
Precentral	70–100	Motor
Precentral	55–70	Sensory
Postcentral	70–100	
Postcentral	55–70	
Superior parietal	70–100	
Inferior parietal	45–70	Superior parietal
Precuneus	65–80	Inferior parietal
Cuneus	45–65	Occipital
Calcarine	30–45	
Lingual	15–30	
Superior temporal	30–45	Superior tem-
Middle temporal	15–30	poral
Anterior medial temporal	20–35	Medial temporal
Posterior medial temporal	20–35	Deep gray
Inferior temporal	5–20	
Caudate nucleus	35–55	
Lenticular nucleus	35–55	
Thalamus	40–50	Cerebellum
Insular cortex	40–60	
Cerebellum	5–15	

[†] Brain regions are analyzed using a standard atlas, as described by Duara, Margolin, Robertson-Tchabo, et al. 1983 (Ref. 10).

[†] Levels above the inferior orbito-meatal line as described by Duara, Margolin, Robertson-Tchabo, et al. 1983 (Ref. 10).

30-min period. This is one of the subjects of a validation study in preparation.

The kinetic model described here requires extensive validation. With the preliminary data presented, we have demonstrated that two specific behavioral tasks, repeated in the same subjects, yielded virtually identical results (i.e., mean delta percent and s.d. are 1.4% and 6.2% for PPT–PPT, 2.0% and 4.2% for WFT–WFT). Conversely, when different behavioral tasks were used, different metabolic patterns were obtained among tested subjects, and the changes occurred in the expected directions. For example, WFT was expected to activate the frontal lobe relative to PPT, whereas, PPT was expected to activate the occipital lobe relative to WFT. These changes did, indeed, occur to the extent of ~10% in the premotor lobule, 6% in the prefrontal lobule, and 10% in the occipital lobe.

We have made the assumption that rate constant alterations occur instantaneously from one behavioral state to another. Thus, we are able to formulate the tracer amount, $R^*(T_2:T_1)$, for any time after the completion of the first state, based on the simple three-

compartmental model. In reality, the rate constants are likely to adjust to their new values gradually, although the real rate of change is not known. However, if the change in the value of the rate constants occurs in a time period considerably less than the duration of the behavioral state (30 min), then the error caused by the assumption of rapid alteration of rate constants will be small.

By using average rate constant values to obtain $\bar{R}^*(T_2:T_1)$, and therefore $\bar{C}_s^*(T_2:T_1)$, the calculated rCMRglc for the second state may be subject to additional errors over and above the errors that have been reported for the deoxyglucose method (4,6,17). Preliminary error analyses, however, suggest that the accuracy of $\bar{R}^*(T_2:T_1)$ is not very sensitive to errors in rate constants; the error sensitivity of $\bar{R}^*(T_2:T_1)$ to each rate constant, expressed as the percentage error in $\bar{R}^*(T_2:T_1)$ caused by a 1% error in the respective rate constants, is ~ 0.00% for k_1 , -0.07% for k_2 , 0.07% for k_3 , and -0.14% for k_4 . Also, the second injection of FDG can considerably reduce the relative contribution of $R^*(T_2:T_1)$ to $C^*(T_2)$. Based on these preliminary error analyses, we suggest that under the proposed PET schedule, $\bar{C}_s^*(T_2:T_1)$ is subject to a s.d. of error of 4% of true $C_s^*(T_2:T_1)$, and rCMRglc is subject to a s.d. of error of 6% of true rCMRglc(2), from the use of erroneous rate constants.

Another source of error in this method arises from the scanning procedure, itself. Because the behavioral state is ill defined during the 20 min of scanning, the metabolic pattern resulting from the behavioral state gets diluted by the pattern from the behavioral state during scanning. Improvements in PET technology with higher sensitivity scanners will allow shorter scanning times and less error caused by this effect.

The possibility that rate constants for glucose transport could vary from one individual to another and even within the same individual from one time to another time makes the comparison of rCMRglc values obtained from the operational equations subject to relatively large errors. This method of studying the same subject repeatedly, 50 min apart, has the advantage of minimizing these errors within individuals.

Aside from the possible methodologic errors that have been mentioned, other factors could also affect the measured results. These include the statistical errors of measuring tracer concentration using the PET scanner, the error of blood glucose measurement, the error in determining the plasma tracer concentration, and the error induced by variation in the behavioral state resulting from habituation, fatigue, and anxiety. The total error that we have measured in our reproducibility studies is the sum of these errors and the errors from the mathematic model.

Exact repositioning between the two scans is essential in this double activation/double injection method to

correctly calculate rCMR_{glc} of second state. However, exact repositioning is a necessary condition for intra-individual comparisons using any method and is not a new constraint on this method.

Although it is probably true that by using [¹¹C]DG, rather than FDG, the error in calculated rCMR_{glc} values for the second state could be reduced, certain disadvantages in using [¹¹C]DG outweigh the benefits. The shorter half-life of ¹¹C necessitates separate cyclotron and chemistry runs for each injection of [¹¹C]DG. Hence, it is much more cumbersome to use [¹¹C]DG for double studies.

It should be recognized that the changes in regional metabolism reported here are those obtained by a low-resolution PET camera. Owing to partial-volume, our camera considerably underestimates the true extent of regional changes (18). Localized changes in rCMR_{glc}, of a much greater magnitude than the 6%–12% changes reported here, are likely.

In summary, it is possible to obtain data for two behavioral states from a single PET study using two injections of [¹⁸F]fluorodeoxyglucose. The method appears to give reliable metabolic data for the second state, as well as the first, and has significant potential for demonstrating the relationships between behavior and regional cerebral metabolism.

ACKNOWLEDGMENTS

The authors thank Drs. Manuel Viamonte and Albert Gilson for their support, the Mount Sinai Medical Center Radiochemistry and Cyclotron staff for production of the radiochemicals used in this study, Drs. Nathaniel Alpert and Stanley Rapoport for reviewing the manuscript, and Cindy Siegel and Richard Adams for their technical assistance.

This work was made possible by research funds from the Mount Sinai Medical Center, Miami Beach, FL 33140.

REFERENCES

1. Sokoloff L, Reivich M, Kennedy C, et al. The [¹⁴C] deoxyglucose method for the measurement of local cerebral glucose utilization: theory, procedure and normal values in the conscious and anesthetized albino rat. *J Neurochem* 1977; 28:897–916.
2. Reivich M, Kuhl D, Wolf A, et al. The [¹⁸F]fluorodeoxyglucose method for the measurement of local cerebral glucose utilization in man. *Circulation Res* 1979; 44:127–137.
3. Phelps ME, Huang SC, Hoffman EJ, et al. Tomographic measurement of local cerebral glucose meta-

bolic rate in humans with (F-18) 2-fluoro-2-deoxy-D-glucose: validation of method. *Ann Neurol* 1979; 6:371–388.

4. Huang SC, Phelps ME, Hoffman EJ, et al. Non-invasive determination of local cerebral metabolic rate of glucose in man. *Am J Physiol* 1980; 238:E69–E82.
5. Duara R, Gross-Glenn K, Sevush S, et al. Intra-individual and inter-individual variability in cerebral glucose metabolism in the resting state and during psychological activation. *J Cereb Blood Flow Metab* 1985; 5 (suppl 1):S217.
6. Hutchins GD, Holden JE, Koeppe RA, et al. Alternative approach to single-scan estimation of cerebral glucose metabolic rate using glucose analogs with particular application to ischemia. *J Cereb Blood Flow Metab* 1984; 4:35–40.
7. Tewson T. Synthesis of no-carrier-added fluorine-18 2-fluoro-2-deoxy-D-glucose. *J Nucl Med* 1983; 24:718.
8. Vora MM, Boothe TE, Finn RD, et al. Multimilligram preparation of 2-[¹⁸F]-fluoro-2-deoxy-D-glucose via nucleophilic displacement with fluorine-18 labelled fluoride. 1. Purification and quality control procedures. *J Label Compds Radiopharm* 1985; 22:953.
9. Shiue C-Y, Fowler JS, Wolf AP, et al. Gas-liquid chromatographic determination of relative amounts of 2-deoxy-2-fluoro-D-glucose and 2-deoxy-2-fluoro-D-mannose synthesized from various methods. *J Label Compds Radiopharm* 1985; 22:503.
10. Duara R, Margolin RA, Robertson-Tchabo EA, et al. Resting cerebral glucose utilization as measured with positron emission tomography in 21 men between the ages of 21 and 83 years. *Brain* 1983; 106:761–775.
11. Pendleton MG, Heaton RK, Lehman RW, et al. Diagnostic utility of the Thurstone Word Fluency Test in neuropsychological evaluations. *J Clin Neuropsychology* 1982; 4:307–317.
12. Borkowski JG, Benton AL, Spreen O. Word fluency and brain damage. *Neuropsychologia* 1967; 5:135–140.
13. Milner B. Some effects of frontal lobotomy in man. In: *The frontal granular cortex and behavior*, Warren JM, Akert K, eds. New York: McGraw-Hill, 1964.
14. Perrett E. The left frontal lobe of man and the suppression of habitual responses in verbal categorical behavior. *Neuropsychologia* 1974; 12:323–330.
15. Sheremata WA, Siddharthen R, Duara R, et al. Activation of frontal cortex by the verbal fluency task: a positron emission tomography (PET) study. *Neurology* 1985; 35 (suppl 1):97.
16. Duara R, Chang JY, Barker W, et al. Correlation of regional cerebral metabolic activation to performance in activating tasks. *Neurology* 1986; 36 (suppl 1): 349.
17. Brooks RA. Alternative formula for glucose utilization using labeled deoxyglucose. *J Nucl Med* 1982; 23:538.
18. Mazziotta JC, Phelps ME, Plummer D, et al. Quantitation in positron emission computed tomography. 5. Physical-anatomical effects. *J Comput Asst Tomogr* 1981; 5:734–743.